

An Active Functionally Graded Piezocomposite Plate Subjected to a Stochastic Pressure

Marek PIETRZAKOWSKI

*Institute of Machine Design Fundamentals, Warsaw University of Technology
Narbutta 84, 02-524 Warszawa, Poland; e-mail: mpi@simr.pw.edu.pl*

(received October 9, 2014; accepted January 20, 2015)

In the paper the analysis of random vibration of an actively damped laminated plate with functionally graded piezoelectric actuator layers is presented. The simply supported plate is subjected to stochastic loading represented by a uniformly distributed pressure. The random input is assumed as a Gaussian stationary and ergodic process. The actuators are regarded as a multi-layer structure arranged of piezofiber composite sub-layers. The sub-layers differ each other with amount of PZT (lead-zirconate-titanate) fibers and are stacked to achieve a desired change of the PZT volume fraction through the actuator thickness. The gradation scheme of constituents and material properties are estimated by parabolic and power functions. Numerical simulations are performed to recognize the influence of the applied random excitations and the actuator properties gradations on the characteristics of the stochastic field of active plate deflection i.e. power spectral density, autocorrelation function and variance.

Keywords: laminated plate, piezoceramic control, functionally graded actuator, stochastic pressure.

1. Introduction

In the last decades flat piezoelectric transducers have found use for shape and vibration control of thin walled flexible structures. A brittle nature of monolithic PZT (lead-zirconate-titanate) piezoceramics, typically used for actuation because of their high electromechanical efficiency, makes them vulnerable to accidental breakage as well as cracks caused by the host structure curvature related to the operational loads. A way to overcome these drawbacks is to use active composites with PZT fibers surrounded by a polymeric matrix. Firstly this concept was developed at MIT where round PZT fibers were applied. This type of composites known as piezoelectric fiber composites (PFCs) were investigated and presented by BENT *et al.* (1995) for the d_{31} mode actuation and then by BENT and HAGOOD (1997) for the stronger d_{33} mode actuation. In this case interdigitated (ID) electrodes were used to direct the electric field in the fiber direction. The next modification has been developed at NASA (WILKIE *et al.*, 2000). The proposed macro fiber composites (MFCs) are reinforced with rectangular fibers diced from a regular piezoceramic sheet. They are manufactured for both the d_{31} and d_{33} operation modes by Smart Material Corp. WILLIAMS *et al.*

(2002) introduce a discussion of manufacturing process, intended applications and advantages of types of fiber composite actuators. The active plate behaviour with PFC actuator layers was analysed by PIETRZAKOWSKI (2003; 2006) where the vibration control effectiveness was compared depending on the piezocomposite spatial configuration and the fiber volume fraction. The optimisation of the ID electrodes design for active fiber composites was performed using finite element analysis by BOWEN *et al.* (2006).

In order to achieve satisfactory control effectiveness relatively large deformations of piezoelectric actuators have to be generated during the control process. Interaction between the piezoelectric layers and the host structure creates great interlayer shear stresses. Besides, a significant change in elastic properties of bonded or embedded piezoceramic actuators and the host structure material also enhance the shear stress concentration. Recently, the functionally graded material concept has been explored in piezoceramic composites to improve their operational reliability and durability. Usually, elastic and piezoelectric properties are graded along the thickness of functionally graded piezoelectric materials (FGPMs) by changing the volume fraction of constituents. The static transverse displacements and stress field in FGPM laminates com-

posed of layers whose electromechanical properties vary from layer to layer was analysed by ALMAJID *et al.* (2001). Design of bimorph piezocomposite functionally graded actuators was discussed by TAYA *et al.* (2003). The dynamic stability analysis of the FGPM plate under the time-dependent thermal load is presented by TYLIKOWSKI (2004). WANG (2004) introduced finite element modelling for the static and dynamic analysis of the FGPM bimorph. The effects of continuous exponential gradation of the constituents on the FGPM actuator properties and the structural response of the plate are examined by the author (PIETRZAKOWSKI, 2008). He also studied the vibration control of laminated plates using multi-layer functionally graded PFC actuators (PIETRZAKOWSKI, 2012).

The objective of the present study is to analyse random vibration of an actively damped laminated plate comprised classic layers, piezoelectric sensor layers and FGPM actuator layers. The simply supported plate is subjected to stochastic loading represented by a uniformly distributed pressure, which may be treated as an acoustic pressure. The random input, which is assumed as a Gaussian stationary and ergodic process, is defined by a power spectral density (PSD) or correlation function. The FGPM actuators are characterised by almost continuous gradation of elastic and piezoelectric properties along their thickness. They are regarded as a multi-layer structure arranged of composite sub-layers with piezoceramic PZT fibers aligned in-plane within a polymer-based matrix. The sub-layer, which differ each other with amount of PZT fibers, are stacked to achieve a desired change of the PZT volume fraction through the actuator thickness. Two distributions, which estimate the gradient of constituents and material properties, are applied: parabolic function and power function.

The response of the considered plate is a stationary second-order process of the plate deflection whose statistical characteristics can be obtained due to the spectral/correlation analysis (LIN, 1995). Numerical simulations are performed to recognize the influence of the applied random excitations and the actuator properties gradations on the characteristics of the stochastic field of active plate deflection i.e. power spectral density, autocorrelation function and variance.

2. Modelling of the system and theoretical formulation

The system considered herein is a thin rectangular symmetrically laminated plate modelled basing on the Kirchhoff hypotheses. The plate consists of classic orthotropic layers integrated with piezoelectric sensor layers and FGPM actuator layers. Active layers operate in a closed loop with constant gain velocity feedback. It is assumed that the sensor layers made

of monolithic material (e.g. PVDF – polyvinylidene fluoride) are polarized transversally while the composite multi-layer actuators, which produce the bending action, are polarized along the piezoceramic fibers to achieve an increased control effect. This advantage of the d_{33} mode actuation results from higher values of the piezoelectric coefficient d_{33} comparing with the coefficient d_{31} , which is characteristic for transversal polarization. The ID electrodes designed with finger-like sections of alternating polarity are used to direct the electric field along the fibers. The plate is subjected to a stochastic transverse loading uniformly distributed over the plate surface. As mentioned earlier a stationary and ergodic process is supposed.

2.1. Sensor and actuator relations

The voltage signal generated by the sensor can be derived from the constitutive law of direct piezoelectric effect. The governing equation referred to the sensor layer polarized conventionally across its thickness along the 3-axis and with the in-plane material axes 1 and 2 parallel, respectively, to the plate x and y axes has the form

$$D_3 = \mathbf{e}^T \boldsymbol{\varepsilon} + \epsilon_{33} E_3, \quad (1)$$

where D_3 and E_3 are the electric displacement and the external electric field in the 3-axis direction, respectively, $\boldsymbol{\varepsilon}$ is the in-plane strain representation of sensor layer, $\boldsymbol{\varepsilon} = [\varepsilon_1, \varepsilon_2, \gamma_{12}]^T$ with shear strain γ_{12} , \mathbf{e} denotes the piezoelectric coefficient matrix, $\mathbf{e} = [e_{31}, e_{32}, 0]^T$, ϵ_{33} is the material permittivity constant.

In the case considered the external electric field E_3 can be ignored. Thus, after integrating the charge stored on the electrodes and using the standard relation for capacitance and the geometric relation between strain and transverse displacement of the plate the voltage produced by the k -th sensor layer can be given by the following simplified formula

$$V_s^k = -\frac{t_s z_0^k}{\epsilon_{33} A_s} \mathbf{e}^T \int_0^a \int_0^b [w_{,xx}, w_{,yy}, 2w_{,xy}]^T dx dy, \quad (2)$$

where a and b are the plate and the surface electrode dimensions, A_s is the effective electrode area, t_s denotes the layer thickness, z_0^k indicates the distance of the k -th sensor layer from the laminate midplane, $w(x, y, t)$ is the plate transverse displacement. The subscript comma indicates partial differentiation with respect to the variable after the comma.

The FGPM actuator is modelled as a multi-layer structure with PZT fibers aligned in matrix material. Modification of the electromechanical properties is obtained by the PZT material volume fraction (number of PZT fibers), which is constant for each sub-layer

and graded through the total thickness t_a of the actuator (cf. PIETRZAKOWSKI, 2012). The effective properties of the two-phase composite material of the PFC sub-layer are determined basing on the uniform field method, which is a generalization of the series and parallel mixing rules (BENT *et al.*, 1995; BENT, HAGOOD, 1997). For example the outer PFC sub-layer covered by the ID electrode is shown in Fig. 1.

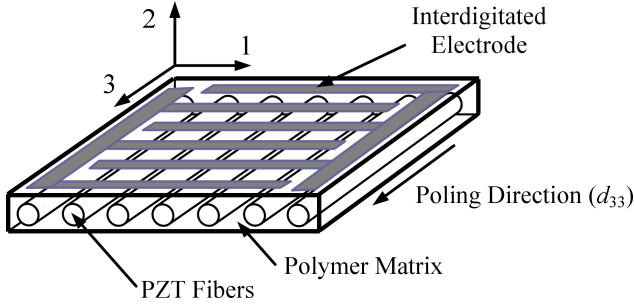


Fig. 1. The construction of the PFC sub-layer equipped with ID electrode.

In general, the actuator performance is described by the constitutive equation of the reverse piezoelectric effect. The constitutive equation reduced to the in-plane material axes 3 and 1 and transformed to the x, y plate reference axes for each PFC sub-layer can be written as

$$\bar{\boldsymbol{\sigma}} = \bar{\mathbf{c}}^{\text{eff}} \bar{\boldsymbol{\varepsilon}} - E_3 \mathbf{R} \mathbf{e}^{\text{eff}}, \quad (3)$$

where $\bar{\boldsymbol{\sigma}} = [\sigma_x, \sigma_y, \tau_{xy}]^T$ and $\bar{\boldsymbol{\varepsilon}} = [\varepsilon_x, \varepsilon_y, \gamma_{xy}]^T$ is the in-plane stress and strain representation, respectively, with shear strain indicated by γ_{xy} , $\bar{\mathbf{c}}^{\text{eff}}$ is the effective stiffness matrix, $\mathbf{e}^{\text{eff}} = [e_{33}^{\text{eff}}, e_{31}^{\text{eff}}, 0]^T$ is the matrix of piezoelectric stress coefficients, E_3 is the electric field along the fibers in the 3-axis direction (see Fig. 1), \mathbf{R} is the transformation matrix related to the skew angle between the piezocomposite material axes 3 and 1 and the plate reference axes x and y .

The effective electromechanical properties mainly depend on the PZT volume fraction, the fiber spatial configuration and electric properties of the matrix material. In the case of multi-layer actuators the effective properties also depend on geometry parameters of the interdigitated electrodes such as the electrode finger width and spacing, and distance between the electrode and the PZT fibers, which determine the length of electric field paths. The path length differs for the particular sub-layer and increases with increasing the distance from the actuator surface electrodes. When the actuator sub-layers are of the same thickness t_p , the averaged path length within each sub-layer can be approximated as

$$l_p^{(i)} = (s + e) + (2i - 1)(1 - v_2)t_p, \quad (4)$$

where s is the electrode spacing, e is the electrode width, v_2 is the constant fraction of piezoceramic ma-

terial measured across the thickness in the 2-axis direction, i indicates the sub-layer number in the sequence from the upper (or lower) electrode to the opposite face, $i = 1, 2, \dots, m$, and m denotes the total number of sub-layers within the FGPM actuator.

Two gradation patterns of the piezoceramic volume fraction across the FGPM actuator are considered. They are approximated by the parabolic function

$$v(z_l) = V_{\max} \left[1 - \left(1 - \frac{1}{R} \right) \left(\frac{2z_l}{(m-1)t_p} \right)^2 \right] \quad (5)$$

and the power function with the exponent r

$$v(z_l) = V_{\max} \left[\frac{1}{R} + \left(1 - \frac{1}{R} \right) \left(\frac{1}{2} + \frac{z_l}{(m-1)t_p} \right)^r \right], \quad (6)$$

where z_l is the local co-ordinate measured from the middle surface of the actuator, R indicates the inhomogeneity parameter which is defined as the ratio of the maximal to minimal piezoceramic volume fractions, $R = V_{\max}/V_{\min}$.

Assuming that the FGPM actuator layers are perfectly integrated with the laminate, the actuation effect being transferred to the main structure may be reduced to the resultant moment distributed along the actuator edges. For further simplification a constant electric field across each sub-layer is supposed and the electric term of the constitutive Eq. (3) is taken into account. When the actuator material axes 3, 1, 2 correspond with the plate axes x, y, z , respectively, a two-dimensional actuation occurs and the resultant bending moment can be written as follows

$$\mathbf{M}^E = \sum_{i=1}^m (\mathbf{e}^{\text{eff}})^{(i)} t_p z_0^{(i)} E_3^{(i)}, \quad (7)$$

where $z_0^{(i)}$ is the distance of the i -th sub-layer from the midplane of the plate, $(\mathbf{e}^{\text{eff}})^{(i)}$ is the effective piezoelectric constant matrix of the i -th sub-layer.

The portion of the electric field $E_3^{(i)}$ supplying the i -th sub-layer depends on the electric path length and when the voltage $V_a(t)$ is applied to the interdigitated surface electrodes the electric field within i -th sub-layer can be approximated by the formula

$$E_3^{(i)} = V_a(t) \left(\frac{1}{l_p^{(i)}} + \frac{1}{l_p^{(m+1-i)}} \right). \quad (8)$$

The voltage V_a driving the actuator is generated by the sensor and then transformed due to the (applied control law) velocity feedback control.

Finally, the control loading $q(x, y, t)$ produced by a pair of actuator layers located symmetrically and operating in bending mode has the form

$$q(x, y, t) = 2 (M_{x,xx}^E + M_{y,yy}^E). \quad (9)$$

In the above relation the twisting moment component vanishes because of a zero skew angle between the plate axes and the piezocomposite material axes assumed.

2.2. Active plate motion and statistic characteristics

Assuming globally orthotropic behaviour, the transverse vibration field $w(x, y, t)$ of the active laminated plate subjected to the random in time uniformly distributed pressure $q(x, y, t)$ can be described by the following equation

$$D_{11}w_{,xxxx} + 2(D_{12} + 2D_{66})w_{,xxyy} + D_{22}w_{,yyyy} + \rho t_c w_{,tt} + q(x, y, t) = p(x, y, t), \quad (10)$$

where D_{ij} ($i, j = 1, 2, 6$) is the element of the bending stiffness matrix, which is complex for a viscoelastic material, t_c and ρ are the total thickness and the equivalent mass density of the plate, respectively, $q(x, y, t)$ is the loading distributed force produced by the piezoelectric control system. The external stochastic plate loading $p(x, y, t)$ can be expressed as

$$p(x, y, t) = p_0(t), \quad (11)$$

where $p_0(t)$ is a stationary and an ergodic Gaussian process.

The input process $p_0(t)$ is defined by the power spectral density $S_{pp}(\omega)$ or autocorrelation function $R_{pp}(t)$.

For the spectral and correlation analysis it is convenient to express the plate dynamic response in terms of a frequency response function (cf. LIN, CAI, 1995). The response of the considered plate system is the stochastic field of the plate deflection whose power spectral density $S_{ww}(x, y, \omega)$ can be determined by the formula

$$S_{ww}(x, y, \omega) = |G_c(x, y, \omega)|^2 S_{pp}(\omega), \quad (12)$$

where $G_c(x, y, \omega)$ is the plate closed-loop frequency response function.

The autocorrelation function of the active plate deflection is calculated according to the Wiener-Khintchine relation

$$R_{ww}(x, y, \tau) = \frac{1}{2\pi} \int_{-\infty}^{\infty} S_{ww}(x, y, \omega) \exp(i\omega\tau) d\omega \quad (13)$$

and the variance of the plate stochastic response can be written as

$$\sigma_w^2(x, y) = \frac{1}{2\pi} \int_{-\infty}^{\infty} S_{ww}(x, y, \omega) d\omega. \quad (14)$$

The closed-loop frequency response function of the actively damped plate can be expressed in the following compact form

$$G_c(x, y, \omega) = \frac{G_{wp}(x, y, \omega)}{1 + G_o(x, y, \omega)}, \quad (15)$$

where G_{wp} is the frequency response function relating the plate deflection to the harmonic in time loading

pressure, G_o is the open-loop frequency response function given as the following product

$$G_o(x, y, \omega) = G_{vw}^s(x, y, \omega)G_d(\omega)G_{wv}^a(x, y, \omega), \quad (16)$$

where G_{vw}^s is the frequency function of sensor voltage to plate deflection, G_{wv}^a is the frequency response function of output plate deflection to input actuator voltage, G_d is the controller function which for velocity feedback with the gain factor k_d transforms the voltage signal according to the formula $G_d(\omega) = ik_d\omega$.

Assuming simply supported boundary conditions and applying the closed loop control with velocity feedback, the steady-state solution to the governing Eq. (10) gives the frequency response function, Eq. (15), which describes the active plate transverse vibration desired for the further analysis.

Two types of zero-mean stationary stochastic processes are considered in the study. The first is the process characterized by a constant spectral density within a limited bandwidth. The following power spectral density defines this process

$$S_{pp}(\omega) = S_0 (H(\omega - \omega_1) - H(\omega - \omega_2))$$

(17)

with $S_0 = \frac{\pi \sigma_p^2}{\omega_2 - \omega_1}$,

where ω_1 and ω_2 are the frequency limits, σ_p^2 is the variance.

The second plate loading is assumed as the narrow band stochastic process defined by the following autocorrelation function

$$R_{pp}(\tau) = \sigma_p^2 e^{-\lambda|\tau|} \left(\cos(\beta\tau) - \frac{\lambda}{\beta} \sin(\beta|\tau|) \right), \quad (18)$$

where β and λ are the process parameters.

The power spectral density due to the Fourier transform can be written as

$$S_{pp}(\omega) = \frac{\sigma_p^2 \omega^2}{(\omega^2 - \lambda^2 - \beta^2)^2 + 4\lambda^2 \omega^2}. \quad (19)$$

The parameter β is responsible for a predominant frequency of the process spectrum.

3. Results and discussion

In calculations a simply supported cross-ply laminated plate of dimensions $400 \times 400 \times 2$ mm is considered. The plate consists of orthotropic graphite-epoxy layers, PVDF sensors and FGPM actuator layers of thickness $t_l = 0.15$, $t_s = 0.1$ and $t_a = 0.6$ mm, respectively. The layers are stacked according to the symmetric order $[S/A/0^\circ/90^\circ]_s$, where “S” and “A” indicate sensor and actuator, respectively. The FGPM actuator is regarded as being consisted of six piezocomposite sub-layers of the same thickness and the constant effective properties related to the applied distribution

Table 1. Properties of PFC components (BENT, HAGOOD, 1997).

Parameter	ρ [kgm ⁻³]	c_{11} [GPa]	c_{12} [GPa]	c_{13} [GPa]	c_{33} [GPa]	G [GPa]	e_{31} [Cm ⁻²]	e_{33} [Cm ⁻²]	$\epsilon_{33} / \epsilon_0$
PZT-5H	7650	127	80.2	84.7	117	36.3	-4.42	15.5	1392
Matrix	1200	8.15	4.01	4.01	8.15	2.33	0	0	11.2

scheme. The stiffness moduli of the graphite-epoxy composite are assumed as: $Y_{11} = 150$ GPa, $Y_{22} = 9$ GPa, $G_{12} = 7.1$ GPa, and the mass density $\rho = 1600$ kg/m³. The material properties of the PVDF sensor are following: $Y_s = 2$ GPa, $\rho_s = 1780$ kg/m³ and piezoelectric strain constants $d_{31} = 2.3 \cdot 10^{-11}$ mV⁻¹, $d_{32} = 3 \cdot 10^{-12}$ mV⁻¹, which relate to the following stress constants $e_{31} = 4.72 \cdot 10^{-2}$ Cm⁻², $e_{32} = 1.52 \cdot 10^{-2}$ Cm⁻², respectively. The equivalent material damping of the composite plate is described due to the Kelvin-Voigt model. In calculations the following retardation time values: $\mu_1 = 10^{-6}$ s, $\mu_2 = \mu_{12} = 4 \cdot 10^{-6}$ s for orthotropic graphite-epoxy layers, $\mu_s = 2 \cdot 10^{-6}$ s for PVDF layers and $\mu_m = 8 \cdot 10^{-6}$ s for matrix material of the FGPM actuator are used. The electromechanical properties of components of the piezocomposite actuator are listed in Table 1.

The PZT material gradation across the actuator is approximated by the parabolic function (Eq. (5)) with the maximal PZT volume fraction V_{max} in the middle of the actuator layer, and the power function (Eq. (6)) with the exponent $r = 3$ and the electro-elastic properties decreasing towards the middle surface of the plate.

For example, Fig. 2 shows the approximated variation of the effective piezoelectric coefficient e_{33}^{eff} through the thickness direction obtained for the parabolic and power gradation patterns, respectively, assuming that the inhomogeneity parameter is $R = 10$.

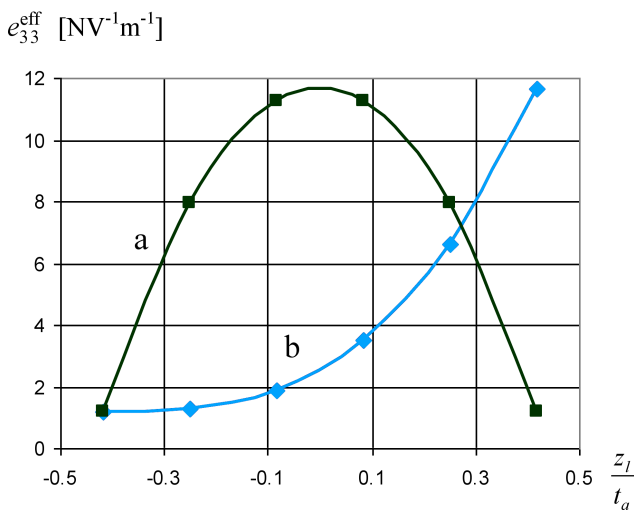


Fig. 2. Approximated gradation of the effective piezoelectric coefficient values across the FGPM actuator: (a) the parabolic gradation, (b) the power gradation law ($r = 3$).

Firstly, the plate is loaded by the random pressure described according to the PSD formula, Eq. (17), as the stochastic process with the constant spectral density within the frequency limits $\omega_1 = 100$ s⁻¹ and $\omega_2 = 950$ s⁻¹ and the standard deviation $\sigma_p = 100$ Pa. For the input process the one-sided PSD function and autocorrelation function for $\tau \geq 0$ are shown in Fig. 3.

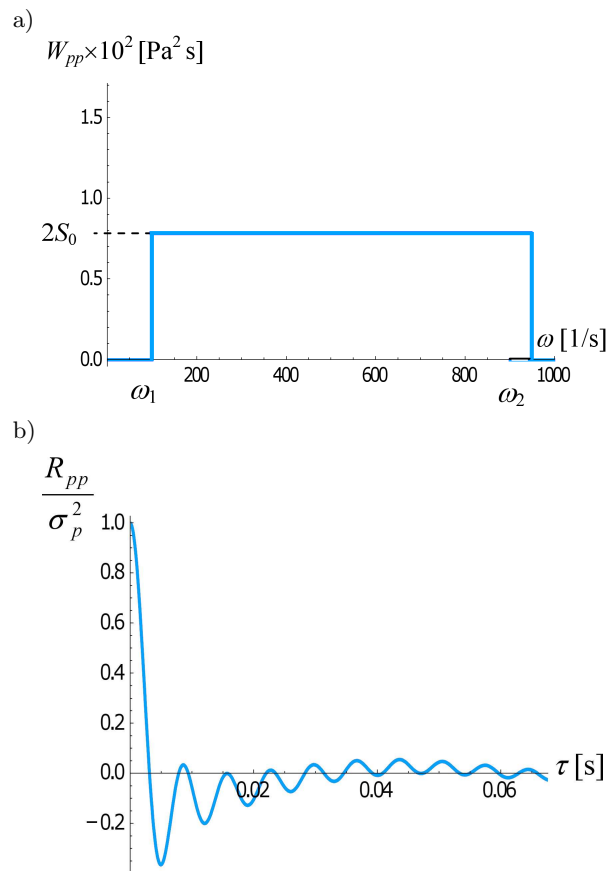


Fig. 3. The input wide band process characteristics: a) one-sided PSD, b) normalized autocorrelation function.

Considering the parabolic gradation scheme of the actuator properties (with the inhomogeneity parameter $R = 10$), the influence of the control gain factor k_d on the one-sided PSD and the normalized autocorrelation function of the active plate deflection process are presented in Fig. 4. In the study calculations of the plate transverse displacement characteristics are performed at the selected point of co-ordinates $x, y = 0.1$ m. With increasing the control gain factor a significant reduction of the spectral density values and the correlation time can be observed. A stronger

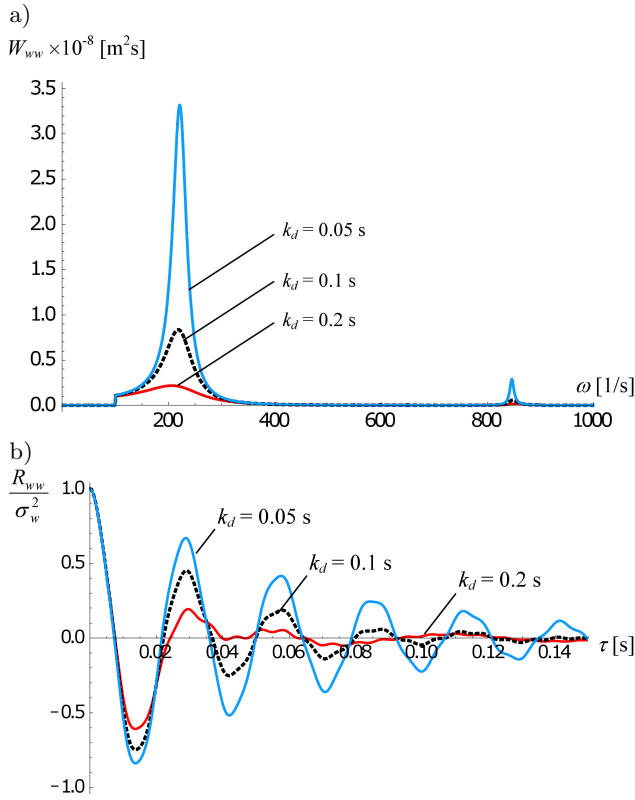


Fig. 4. The input wide band process. Influence of the control gain factor on the statistic characteristics of the active plate deflection: a) one-sided PSD, b) normalized autocorrelation function.

active damping of the plate vibration creates these effects. But it should be noted, however, that in the case of velocity feedback the control gain must be limited to protect the actuator from overdriving and unstable behaviour of the system. Because of a relatively wide frequency band of the random excitation (including the second natural frequency) the influence of the second vibration mode on the characteristics of the plate response occurs. A disturbance of the autocorrelation function and the next peak in the spectral density plot can be noticed.

In Fig. 5 the comparison of statistic characteristics related to the parabolic gradation and the power gradation ($r = 3$) of the actuator properties is shown. In the case of the gradation based on the power low, greater values of both the predominant frequencies and the power spectral density are noticed. An increase in the power spectral density values means lower control effectiveness.

Next Fig. 6 shows the variance of the plate deflection versus the control gain factor depending on the actuator properties gradation. The variance diagrams start with extremely large values and a significant slope for low control gains and changes slightly when the gain values become greater. As expected greater values of the variance of the plate displacement are obtained for the power gradation of material properties.

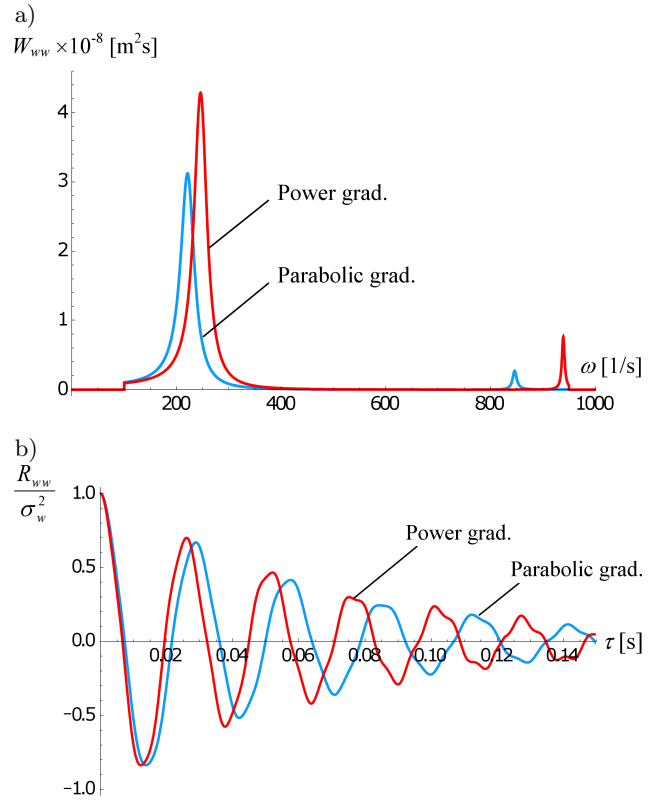


Fig. 5. The input wide band process. Comparison of the statistic characteristics of the active plate deflection depending on the actuator properties gradation scheme ($k_d = 0.05$ s).

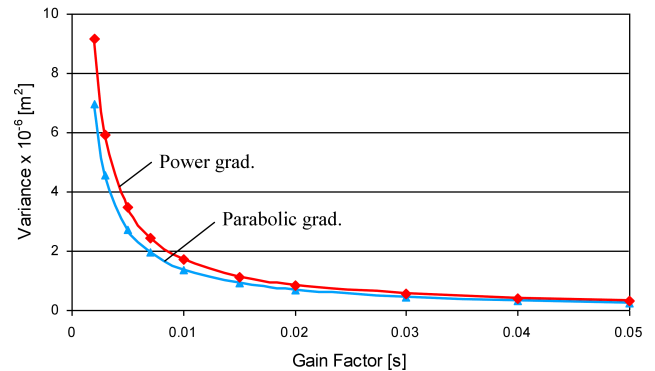


Fig. 6. The input wide band process. Variance of the plate deflection versus the control gain factor depending on the actuator properties gradation scheme ($k_d = 0.05$ s).

The second plate loading is assumed as the narrow band stochastic process defined by the autocorrelation function given by Eq. (17) with the parameters $\lambda = 25$, $\beta = 250$ and $\sigma_p = 100$ Pa. The one-sided PSD and autocorrelation function are shown in Fig. 7. The predominant frequency of the input process is close to the first natural frequency of the plate.

The diagrams presented in Fig. 8 confirm the influence of the control gain factor on the power spectral density and the autocorrelation function of the plate

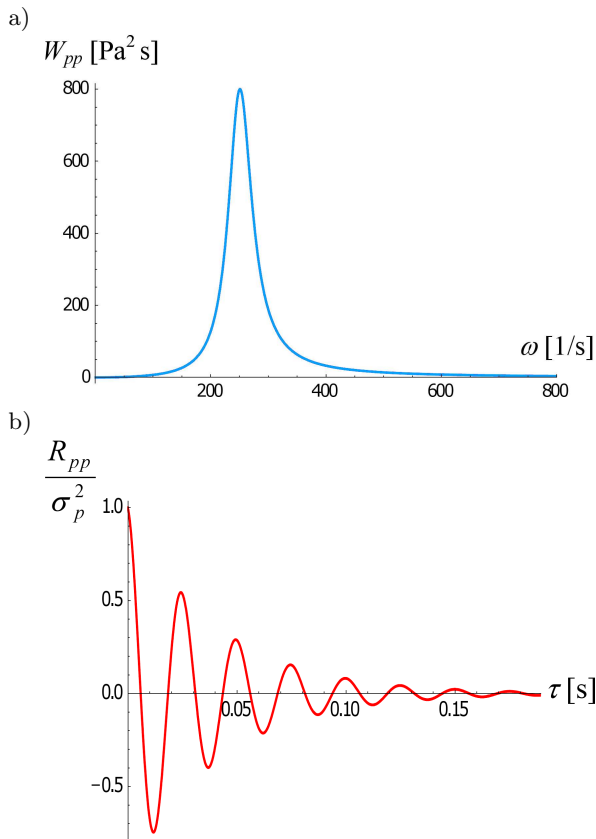


Fig. 7. The input narrow band process characteristics: a) one-sided PSD, b) normalized autocorrelation function.

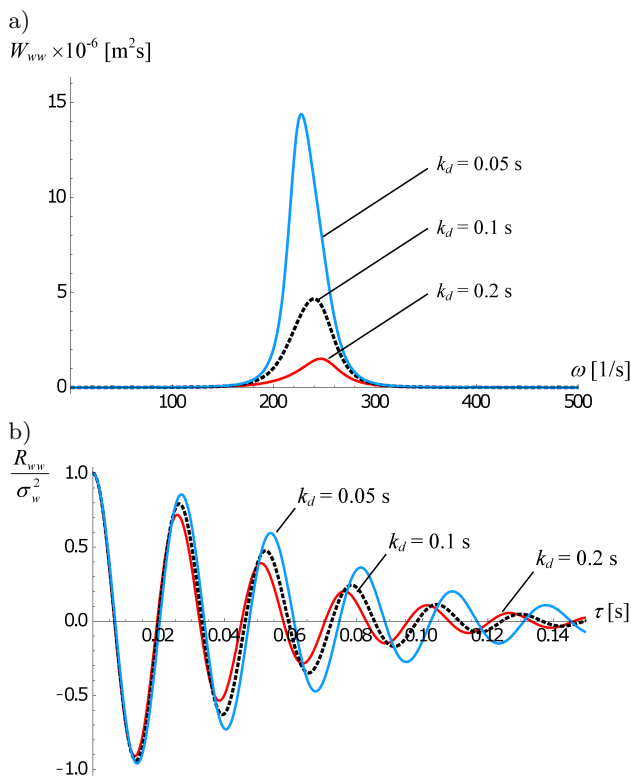


Fig. 8. The input narrow band process. Influence of the control gain factor on the statistic characteristics of the active plate deflection: a) one-sided PSD, b) normalized autocorrelation function.

displacement. Now, because of the predominant frequency range, which characterizes the excitation, a disturbance of the autocorrelation function induced by the higher vibration modes is not observed.

In Fig. 9 the one-sided PSD functions and the normalized autocorrelation functions of the plate stochastic response to the narrow band input process calculated for the parabolic and power ($r = 3$) gradation of the actuator properties are compared.

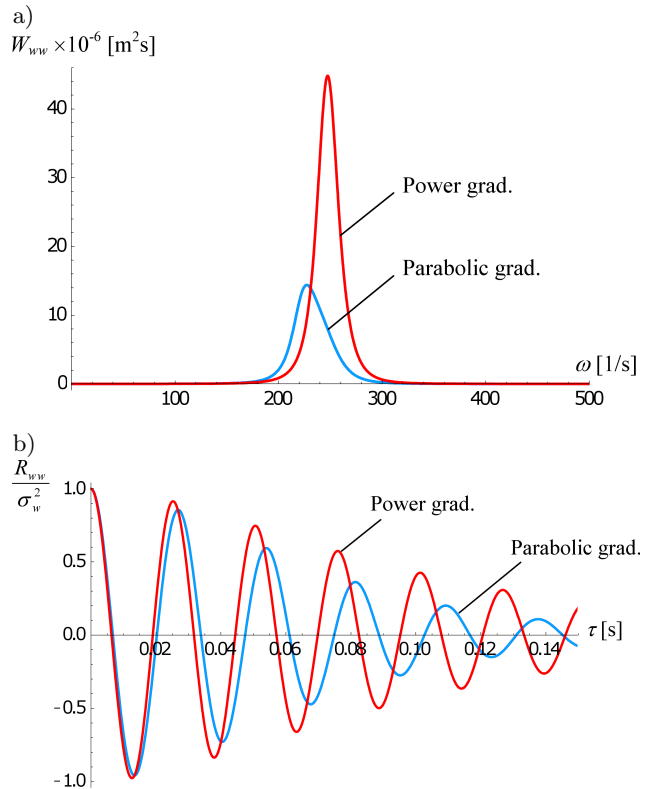


Fig. 9. The input narrow band process. Comparison of the statistic characteristics of the active plate deflection depending on the actuator properties gradation scheme ($k_d = 0.05$ s).

The comparison of the statistic characteristics of the active plate response depending on the applied pattern of the actuator properties gradation shows that in the case of the narrow band input process, the values of the compared plots differ significantly. It means that decreasing of the control effectiveness is more evident when the power law of properties gradation is applied. This effect can be clearly seen comparing plots of the variance versus the control gain factor presented in Fig. 10.

Thus, it is confirmed that the parabolic scheme of the actuator properties gradation because of amount of piezoceramic fibers offers better control effectiveness comparing with the gradation described by the power function.

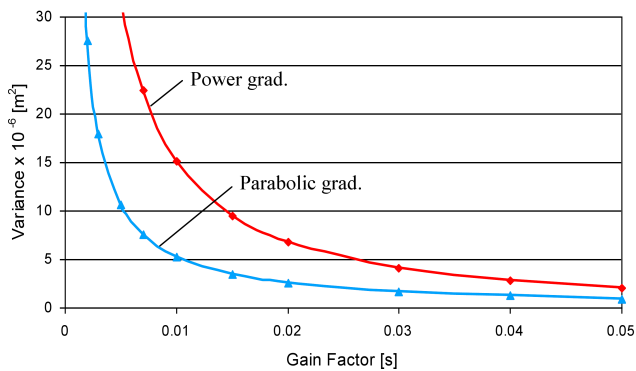


Fig. 10. The input narrow band process. Variance of the plate deflection versus the control gain factor depending on the actuator properties gradation scheme ($k_d = 0.05$ s).

4. Conclusions

The model of the multi-layer actuator with gradation of electromechanical properties has been formulated and applied for the stochastic analysis of the transverse vibration control of laminated plate loaded by the stochastic pressure. The performed calculations concern statistic characteristics of the plate deflection process.

Generally, the first natural frequency dominates in the output spectral density and correlation functions obtained for the applied random excitations. But in the case of the wide band input process the effect of higher vibration modes on the plate deflection stochastic field occurs.

The results of simulations show the influence of the applied piezoelectric material gradation scheme and the control gain factor on the active plate power spectral density, correlation function and variance, and also the control system effectiveness. Based on the obtained statistic characteristics it is exposed that the actuator layer with parabolic law of properties gradation offers better control effectiveness comparing with that of the applied power law gradation.

It is proved that with increasing the control gain factor both the variance and the correlation time of the plate response are decreased and the influence of the gain factor on the characteristics becomes significantly weaker for its greater values.

References

1. ALMAJID A., TAYA M., HUDNUT S. (2001), *Analysis of out-of-plane displacement and stress field in a piezo-composite plate with functionally graded microstructure*, International Journal of Solids and Structures, **38**, 3377–3391.

2. BENT A.A., HAGOOD N.W., RODGERS J.P. (1995), *Anisotropic actuation with piezoelectric fiber composites*, Journal of Intelligent Material Systems and Structures, **6**, 338–349.
3. BENT A.A., HAGOOD N.W. (1997), *Piezoelectric fiber composites with interdigitated electrodes*, Journal of Intelligent Material Systems and Structures, **8**, 903–919.
4. BOWEN C.R., NELSON L.J., STEVENS R., CAIN M.G., STEWART M. (2006), *Optimisation of interdigitated electrodes for piezoelectric actuators and active fibre composites*, Journal of Electroceramics, **16**, 263–269.
5. LIN Y.K., CAI G.Q. (1995), *Probabilistic structural dynamics: advanced theory and applications*, McGraw-Hill, Inc., New York.
6. PIETRZAKOWSKI M. (2003), *Composites with piezoceramic fibers and interdigitated electrodes in vibration control*, Mechanics Quarterly AGH, **22**, 3, 375–380.
7. PIETRZAKOWSKI M. (2006), *Dynamic effects of material damping in active laminated reinforced with piezoceramic fibers*, Engineering Transactions, **54**, 3, 223–231.
8. PIETRZAKOWSKI M. (2008), *Vibration reduction of laminated plates with various piezoelectric functionally graded actuators*, Proceedings of 9th Biennial ASME Conference on Engineering Systems Design and Analysis ESDA2008, Paper No. 59271, pp. 255–261, Haifa.
9. PIETRZAKOWSKI M. (2012), *Modelling of piezocomposite functionally graded plates for active vibration control*, Proceedings of the XI Int. Conf. on Computational Structures Technology, B.H.V. Topping [Ed.], Civil-Comp Press, Paper No. 45, pp.1–13, Dubrovnik.
10. TAYA M., ALMAJID A., DUNN M., TAKAHASHI H. (2003), *Design of bimorph piezo-composite actuators with functionally graded microstructure*, Sensors Actuators A, **107**, 248–260.
11. TYLIKOWSKI A. (2004), *Stability of functionally graded plate under in-plane time-dependent compression*, Mechanics and Mechanical Engineering, **7**, 2, 5–12.
12. WANG S.Y. (2004), *A finite element model for the static and dynamic analysis of a piezoelectric bimorph*, International Journal of Solids and Structures, **41**, 4075–4096.
13. WILLIAMS B.R., PARK G., INMAN D.J., WILKIE W.K. (2002), *An overview of composite actuators with piezoceramic fibers*, Proceedings of 20th International Modal Analysis Conference (IMAC), pp. 4–7, Los Angeles.
14. WILKIE W.K., BRYANT R.G., HIGH J.W., FOX R.L., HELLBAUM R.F., JALINK A., LITTLE B.D., MIRICK P.H. (2000), *Low-cost piezocomposite actuator for structural control applications*, Proceedings of SPIE 3991, Smart Structures and Materials 2000: Industrial and Commercial Applications of Smart Structures Technologies, pp. 323–334, Newport Beach.